Structural and optical properties of wurtzite $Mg_xZn_{1-x}S$ ($0 \leqslant x \leqslant 0.25$) films grown on (0001) Al_2O_3 by pulsed-laser deposition

H. C. Ong[a)]
Department of Physics, The Chinese University of Hong Kong, Shatin, Hong Kong

J. Y. Dai
Department of Applied Physics, Hong Kong Polytechnic University, Hong Kong

(Received 22 October 2001; accepted for publication 27 June 2002)

Wurtzite $Mg_xZn_{1-x}S$ ($0 \leqslant x \leqslant 0.25$) thin films have been epitaxially grown on (0001) Al_2O_3 using pulsed-laser deposition. High-quality films can be prepared at a growth temperature of 450–550 °C with (0001) ω-rocking curve full width at half maximum as narrow as 0.09°. High-resolution cross-sectional transmission electron microscopy of the films deposited at 500 °C shows the presence of the mixture of zinc-blende and wurtzite phases at the interface, and therefore the interfacial region is highly defective. However, above the critical thickness of ~5 nm, the film bulk consists of pure wurtzite material with a very high level of crystallinity. The band edge of $Mg_xZn_{1-x}S$ films examined by transmission spectroscopy at room temperature increases from 3.75 eV at $x=0$ to 3.95 at $x=0.25$. © *2002 American Institute of Physics.* [DOI: 10.1063/1.1502191]

ZnS has found widespread application in photonics because of its band gap of 3.7 eV, the largest among the Zn-based chalcogenides. In addition, quantum confinement can be realized in a ZnS quantum well by using MgZnS alloys as the potential barrier.[1] Due to the small difference in the lattice mismatch, ZnS epilayers have so far been prepared on (100) GaAs and (100) Si substrates, which usually give rise to a zinc-blend (ZB) structure.[2] There is little knowledge concerning the wurtzite (WZ) counterpart despite the fact that WZ III-V nitrides and ZnO have recently been receiving a considerable amount of attention. McGill and his coworkers have attempted to grow ZnS on (0001) Al_2O_3 using molecular beam epitaxy (MBE) followed by thermal annealing.[3] Although the crystallinity of the films improves significantly after the annealing, ZB structure instead of WZ results.

We have grown wurtzite $Mg_xZn_{1-x}S$ ($0 \leqslant x \leqslant 0.25$) on (0001) Al_2O_3 by pulsed laser deposition (PLD) and have studied the structural and optical properties by using x-ray diffraction (XRD), high-resolution transmission electron microscopy (TEM), and transmission spectroscopy. XRD shows that all the films exhibit single c-axis orientation with the full width at half maximum (FWHM) of ω-rocking curve as narrow as 0.09°. Optical absorption has indicated a gradual increase of the band gap with increasing Mg content. However, the presence of a mixed phase of ZB and WZ nuclei at the interface is observed before the growth of pure WZ phase. Possible mechanisms of the phase transformation are discussed.

Thin films of MgZnS are deposited on (0001) Al_2O_3 substrates by PLD at substrate temperatures of 350–550 °C measured by an optical pyrometer.[4] An ArF excimer laser with pulse energy of 80–150 mJ and repetition rate of 8 Hz is employed to ablate a series of commercially available, hot pressed, MgZnS targets. The substrates are first degreased by acetone and methanol followed by a deionized water rinse. They are then etched in hot (160 °C) 3:1 $H_2SO_4:H_3PO_4$ for 2 min. Prior to deposition, the system is evacuated to a base pressure of 1×10^{-7} Torr. Films are either prepared in a high purity H_2S of 1×10^{-5} to 1×10^{-4} Torr ambient or at the base pressure. The texture of the as-deposited films is characterized by XRD at a receiving slit size of 0.2° and the microstructures are examined by cross-sectional TEM. Energy dispersive x-ray (EDX) analysis in the TEM is utilized to examine the Mg content. For the optical measurement, a UV–vis–IR dual beam spectrometer is used to extract the absorption edge of the materials. A bare sapphire substrate is placed in the reference beam so that the conversion of the transmission to absorption can be simplified.[5] All the measurements are carried out at room temperature and immediately after deposition to reduce surface contaminations.

All the films show a single texture in (111) ZB or (0001) WZ orientation in the $\theta/2\theta$ scan, indicating the epitaxial growth. The XRD scans of films deposited at 500 °C are illustrated in Fig. 1(a) for $x=0$, 0.07, 0.2, and 0.25. Because the d-spacing of the (111) ZB plane and the (0001) WZ plane are almost identical, we are unable to distinguish whether the crystal structure is ZB or WZ from the $\theta/2\theta$ scan. However, the TEM examination, which will be presented shortly, reveals the film bulk consists entirely of WZ phase except for a small amount of (111) ZB grains present at the interface where the nucleation occurs. Films prepared at temperature below 450 °C show a broad ω peak of not less than 2°, indicating a relatively poor c-axis alignment with respect to the substrate. High-quality MgZnS films can be grown at temperature of 450–550 °C. The (0001) ω peak profiles of the corresponding MgZnS are shown in Fig. 1(b). In general, they exhibit two superimposed peaks, one narrow and one much broader. The narrow peak has a FWHM of 0.09–0.11° and does not change with the growth temperature. However, the FWHM of the underlying broad peak reduces from 2° to ~1° as the temperature increases from 450 to 500 °C. The feature of two superimposed peaks is a characteristic of dif-

[a)]Electronic mail: hcong@phy.cuhk.edu.hk

Downloaded 22 Mar 2011 to 158.132.161.52. Redistribution subject to AIP license or copyright; see http://apl.aip.org/about/rights_and_permissions

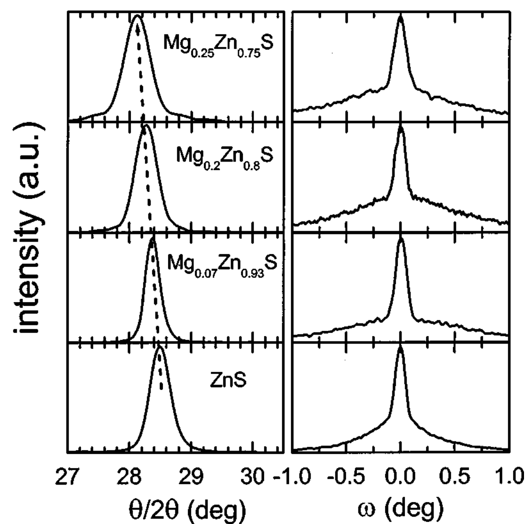

FIG. 1. XRD $\theta/2\theta$ and ω scans of wurtzite $Mg_xZn_{1-x}S$ ($0 \leq x \leq 0.25$) epilayers grown on (0001) Al_2O_3 at 500 °C.

fraction from films that contain two distinct layers of crystallinity. The narrow peak arises primarily from a near-perfect crystalline region where coherent diffraction occurs. On the other hand, a less coherent region where the layer is highly strained or otherwise defective gives rise to the broad component. We have increased the width of the receiving slit from 0.05° to 3° and have observed no change of the broad peak FWHM, although that of the narrow peak is found to increase gradually. This is consistent with the fact that the mosaic spread of crystallites contributes to the broad component whereas the narrow counterpart results from the intrinsic rocking curve at the high quality region.[6]

Figure 2 shows the variation of the c-axis lattice constant as well as two FWHMs of rocking curve as a function of Mg content. A linear dependence of the lattice constant on Mg mole fraction confirms the validity of Vegard's law.[7] However, noting that the lattice constant for the bulk WZ ZnS is 6.26 Å,[8] a slight tensile strain of 0.06% along the c-axis is expected to develop in the film by considering the lattice mismatch between the film and substrate, which is ~7.8%. The tensile strain increases even more at growth temperature above 500 °C, which shows the thermal strain takes over after that temperature. A similar scenario is observed in other MgZnS alloys. By extrapolating the straight line to $x=1$, corresponding to MgS, we reach a value of 6.55 Å. This

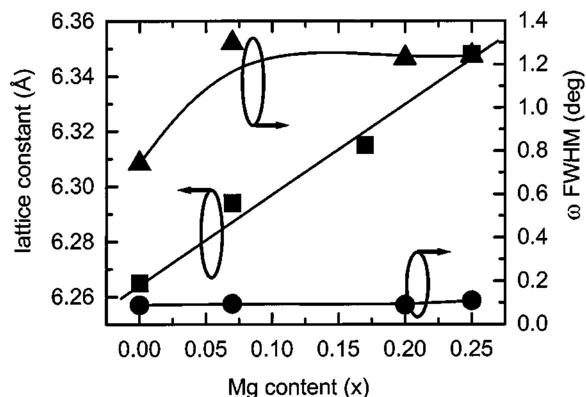

FIG. 2. The c-axis lattice constant and the FWHMs ω-rocking curve are illustrated as a function of Mg content.

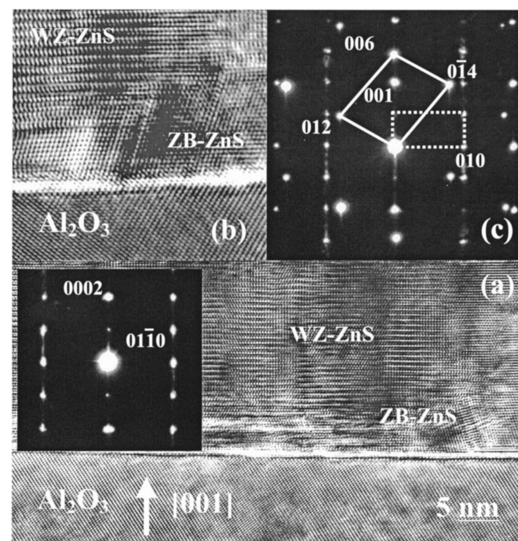

FIG. 3. The cross-sectional TEM image of ZnS grown (a) on sapphire. ZB indicates the presence of zinc-blend ZnS crystalline grains. The enlarged TEM image of the interfacial region, which clearly shows the WZ and ZB stacking sequences (b). The white solid line in the diffraction pattern represents the diffraction of substrate and the white dot line represents the film (c). The corresponding diffraction pattern of film surface confirms the presence of pure wurtzite structure (inset).

value deviates almost 1.7% from the theoretical value of 6.443 Å,[9] and the discrepancy is possibly due to the strain incorporation. The narrow FWHM remains relatively constant with increasing Mg composition, indicating a minor degradation of crystallinity at the surface as a result of alloying. The broad FWHM, on the other hand, increases from 0.74° to 1.2° and saturates thereafter.

Figure 3(a) is a cross-sectional TEM image of ZnS deposited on sapphire. The image illustrates a uniform film with almost atomically smooth surface and sharp interface. No distinctive columnar grain boundary is observed, indicating a good in-plane alignment. Examination of the lattice stacking sequences at the interfacial region shows that two crystalline phases of ZnS are present. The enlarged TEM image [Fig. 3(b)] indicates both the wurtzite and zinc-blend stacking orders occur near the interface. However, the ZB ZnS grains are almost fully transformed to WZ structure when the film is grown above a critical thickness of ~5 nm. Therefore, the film surface contains solely the WZ structure, as indicated by the electron diffraction pattern [inset of Fig. 3(a)]. Except near the interface where ZB ZnS accumulates, stacking faults and twins are rarely seen in the film bulk, in contrast to the ZB ZnS/GaAs in which stacking faults are the major defect conglomeration in the film.[10] However, antiphase boundaries (APB) are frequently observed throughout the film and we believe that they evolve from the three-dimensional nucleation of ZB and WZ ZnS at the interface. Comparing TEM with XRD results, we conclude that the region near the interface is highly defective, due to the lattice mismatch and mixed phases, but the upper part of the layer is of high quality. The electron diffraction pattern [Fig. 3(c)] confirms a heteroepitaxy on Al_2O_3 with the orientation relationship as: (0001) ZnS∥(0001) Al_2O_3 and [1120] ZnS∥ [1120] Al_2O_3. In contrast to GaN[11] and ZnO[12] grown on (0001) Al_2O_3, where 30° rotation of the unit cell with respect to the substrate is observed, our finding indicates a

Downloaded 22 Mar 2011 to 158.132.161.52. Redistribution subject to AIP license or copyright; see http://apl.aip.org/about/rights_and_permissions

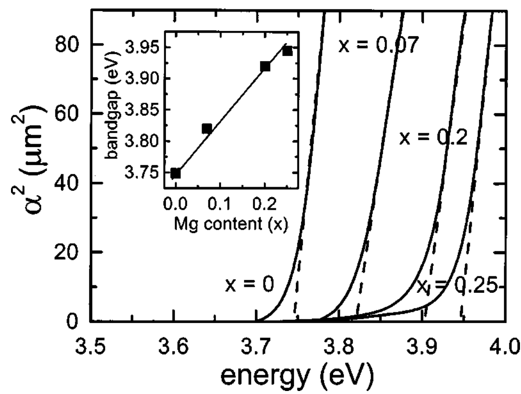

FIG. 4. The band edge of MgZnS films for $x=0$, 0.07, 0.2, and 0.25. The extrapolation of the band edge indicates the value of the band gap. The deduced band gaps are summarized in the inset for various Mg contents.

parallel hexagon-on-hexagon alignment. The cross-sectional TEM image of the MgZnS layer shows a comparable microstructure to the ZnS signifying that a pure crystalline phase is grown. ZB nuclei are also found at the interface. EDX consistently shows a uniform Mg incorporation throughout the entire film bulk.

The absorption spectra for MgZnS alloys are presented in Fig. 4. The band edge is blue-shifted as a function of Mg mole fraction due to the wider band gap of MgS. Summarized in the inset of Fig. 4, the band gap of MgZnS increases almost linearly from 3.75 eV at $x=0$ to 3.95 eV at $x=0.25$. Assuming the band gap of WZ MgS is almost of the same magnitude as that of the ZB phase, which is ~4.47 eV at room temperature,[13] we have observed a very small bowing parameter for the WZ MgZnS. In fact, a negligible bowing parameter has been reported in the class of ZB MgZn-based alloys,[13] which supports our results.

A possible explanation for the phase behavior is now proposed. Stabilization of nonequilibrium phases has been well documented in thin film growth.[14] Typical examples are the epitaxy of ZB GaN on cubic (001) GaAs[15] and ZB AlN on (001) Si,[16] where a relatively thick layer can be grown. Although the growth of ZB ZnS grains at the interface remains unclear, it is generally agreed that not only does the substrate structure take part in controlling the growth kinetics but also other external factors such as the growth temperature, source flux ratio, etc. McGill and his group have shown that ZnS can be grown on (0001) sapphire by MBE but only resulting in a ZB structure.[3] Therefore, instead of the underlying substrate, other variables are more likely to dominate the nucleation and the subsequent growth process. We believe the highly nonequilibrium nature of the laser induced plasma plume, in contrast to the thermal flux produced in MBE, may take on a key role in assisting the growth. The ion bombardment arising from the plume may reduce the overall free energy of the WZ phase over to the more stable ZB structure and provide the necessary conditions for stabilizing the nonequilibrium WZ structure. It has been observed by Cheng *et al.* that a phase transition of GaN from WZ to metastable ZB structure occurs under the radiation of an ion beam.[17] Further studies are underway to clarify the nucleation and growth mechanisms.

In conclusion, $Mg_xZn_{1-x}S$ ($0\leq x\leq 0.25$) thin films have been epitaxially grown on (0001) Al_2O_3 using pulsed laser deposition. Tensile strain is found to incorporate in the films due to the 7.8% lattice mismatch at the interface. However, the FWHMs of the ω-rocking curve do not change much with the alloying showing minor deterioration in crystal quality. All the films exhibit the presence of two distinct layers of crystallinity. Adjacent to the interface, the materials comprise of a mixture of ZB and WZ grains and are therefore highly defective. However, the crystallinity is improved greatly near the surface region where pure WZ phase is present. Notable variation in the band gap has been observed as a function of Mg composition.

The authors are indebted to T.L. Lee for useful discussion on the XRD. This research was supported by the Chinese University of Hong Kong through the RGC Competitive Earmarked Research Grants (CUHK1101/99E), the Direct Grant (2060218) and the NSFC/RGC Joint Research Scheme (N_CUHK 127/99).

[1] T. Saditoh, T. YoB. Urbaszek, C. M. Townsley, X. Tang, C. Morhain, A. Balocchi, K. A. Prior, R. J. Nicholas, and B. C. Cavenett, Phys. Rev. B **64**, 155321 (2001).
[2] N. Lovergine, M. Longo, C. Gerardi, D. Manno, A. M. Mancini, and L. Vasanelli, J. Cryst. Growth **156**, 45 (1996); L. T. Romano, R. D. Bringans, X. Zhou, and W. P. Kirk, Phys. Rev. B **52**, 11201 (1995).
[3] E. C. Piquette, Z. Z. Bandic, J. O. McCaldin, and T. C. McGill, J. Vac. Sci. Technol. B **15**, 1148 (1997); Z. Z. Bandic, E. C. Piquette, J. O. McCaldin, and T. C. McGill, Appl. Phys. Lett. **72**, 2862 (1998).
[4] H. C. Ong and R. P. H. Chang, Phys. Rev. B **55**, 13213 (1997).
[5] L. Balagurov and P. J. Chong, Appl. Phys. Lett. **68**, 43 (1996).
[6] D. B. Cullity, *Elements of X-ray Diffractions* (Addiison-Wesley, Reading, MA, 1978).
[7] T. F. Huang and J. S. Harris, Jr., Appl. Phys. Lett. **72**, 1158 (1998).
[8] *Numerical Data and Functional Relationships in Science and Technology*, Landolt-Bornstein, New Series Group III, edited by K. H. Hellwege and O. Madelung (Springer, New York, 1982), Vols. 17a and 22a.
[9] S. G. Lee and K. J. Chang, Phys. Rev. B **52**, 1918 (1995).
[10] J. M. McCamy, D. H. Lowndes, J. D. Budai, R. A. Zuhr, and X. Zhang, J. Appl. Phys. **73**, 7818 (1993).
[11] K. Dovidenko, S. Oktyabrsky, J. Narayan, V. Joshkin, and M. Razeghi, Mater. Res. Soc. Symp. Proc. **482**, 411 (1998).
[12] J. Narayan, K. Dovidenko, A. K. Sharma, and S. Oktyabrsky, J. Appl. Phys. **84**, 2597 (1998).
[13] H. Okuyama, Y. Kishita, and A. Ishibashi, Phys. Rev. B **57**, 2257 (1998).
[14] R. Bruinsma and A. Zangwill, J. Phys. (France) **47**, 2055 (1986); D. M. Wood and A. Zunger, Phys. Rev. B **40**, 4062 (1989).
[15] J. W. Orton and C. T. Foxon, Rep. Prog. Phys. **61**, 1 (1998).
[16] W. T. Lin, L. C. Meng, G. J. Chen, and H. S. Liu, Appl. Phys. Lett. **66**, 2066 (1997).
[17] L. Cheng, G. Zhang, D. Yu, and Z. Zhang, Appl. Phys. Lett. **70**, 1408 (1997).

Downloaded 22 Mar 2011 to 158.132.161.52. Redistribution subject to AIP license or copyright; see http://apl.aip.org/about/rights_and_permissions